



# A promising protocol for the endothelialization of vascular grafts in an instrumented rotating bioreactor towards clinical application

Sebastian Heene<sup>a,c,1</sup>, Jannis Renzelmann<sup>a,1</sup>, Caroline Müller<sup>a,c</sup>, Nils Stanislawski<sup>b,c</sup>, Fabian Cholewa<sup>b,c</sup>, Pia Moosmann<sup>d</sup>, Holger Blume<sup>b</sup>, Cornelia Blume<sup>a,c,\*</sup>

<sup>a</sup> Leibniz University Hannover, Institute of Technical Chemistry, Callinstr. 5, D-30167 Hannover, Germany

<sup>b</sup> Leibniz University Hannover, Institute of Microelectronic Systems, Architecture and Systems Group, Appelstr. 4, D-30167 Hannover, Germany

<sup>c</sup> Lower Saxony Centre for Biomedical Engineering, Implant Research, and Development (NIFE), Stadtfelddamm 34, 30625 Hannover, Germany

<sup>d</sup> Biotrics Bioimplants AG, Ullsteinstraße 108, D-12109 Berlin, Germany

## ARTICLE INFO

### Keywords:

Endothelialization  
Vascular graft  
Shear stress  
Bioreactor system  
Dynamic cultivation  
Cell alignment

## ABSTRACT

Pre-endothelialization of a tissue-engineered vascular graft before implantation aims to prevent thrombosis and immunoreactions. This work demonstrates a standardized cultivation process to build a confluent monolayer with human aortal endothelial cells on xenogenous scaffolds. Pre-tested dynamic cultivation conditions in flow slides with pulsatile flow (1 Hz) representing arterial wall conditions were transferred to a newly designed multi-featured rotational bioreactor system. The medium was thickened with 1% methyl cellulose simulating a non-Newtonian fluid comparable to blood. Computational fluid dynamics was used to estimate the optimal volume flow and medium distribution inside the bioreactor chamber for defined wall-near shear stress levels. Flow measurements were performed during cultivation for constant monitoring of the process. Three decellularized porcine arteries were seeded and cultivated in the bioreactor over six days. 1% MC turned out to be the optimal percentage to achieve shear stress values ranging up to 10 dyn/cm<sup>2</sup>. Vascular endothelial cells formed a continuous monolayer with significant cell alignment in the direction of flow. The presented cultivation protocol in the bioreactor system thus displays a promising template for graft endothelialization and cultivation. Therefore, establishing a key step for future tissue-engineered vascular graft development with a view towards clinical application.

## 1. Introduction

Cardiovascular diseases (CVDs) such as coronary heart disease are the main cause of mortality worldwide with an estimated 17.8 million deaths in 2017 and the trend continues to rise [1]. Deaths from CVD jumped globally from 12.1 million in 1990–20.5 million in 2021, according to a new report from the World Heart Federation (WHF) [2]. Implantation of a purely synthetic graft implicates concomitant medical treatment with, e.g., anticoagulation or other drugs that benefit the blood composition and anti-atherosclerotic effects. In addition, replacing middle-sized occluded arteries such as coronary arteries affords autologous venous vessels, which might be rare, especially in older patients [3,4]. Thus, bio-artificial vascular substitutes, developed by tissue engineering (TE), are urgently needed.

These tissue-engineered vascular grafts (TEVGs) have to fulfill

several requirements such as high resistance to blood flow and pressure, a tissue matrix with low risk of inflammation, induction of foreign body responses and immune recognition, and offer the possibility of remodeling after implantation as well as an anti-thrombogenic surface. Such biohybrid structures combine the biomechanical properties of a synthetic graft with the biophysical qualities of native blood vessels. TEVGs can rely on a synthetic or xenogenous tubular scaffold, with the latter still bearing a risk of rejection. In contrast, a biodegradable synthetic scaffold can serve as a temporal template for endothelial cells to provide mechanical stability as well as cell adhesive and cell growth-favoring properties. The scaffold will be replaced by the reorganized extracellular matrix after implantation [5].

Implantation of a TEVG is followed by spontaneous seeding in the recipient's body with mononuclear cells and a risk of neo-intima formation and re-occlusion of the graft. Many studies have shown that

\* Corresponding author at: Leibniz University Hannover, Institute of Technical Chemistry, Callinstr. 5, D-30167 Hannover, Germany.

E-mail address: [blume@iftc.uni-hannover.de](mailto:blume@iftc.uni-hannover.de) (C. Blume).

<sup>1</sup> contributed equally to this article

endothelialization before implantation increases the chance for long-term patency of these grafts, and additional dynamic conditioning of the endothelial cells supports an anti-thrombogenic phenotype [6–10]. Thus, the extra-corporal endothelialization of a TEVG in a suitable bioreactor system is essential for the formation of a fully functional TEVG and strengthens cell attachment to the scaffold, preventing cell loss and occlusion after implantation [10].

A pulsatile and dynamic cultivation was shown to have a crucial impact on the formation of a flow-resistant and anti-thrombogenic endothelial cell layer [11]. Using autologous endothelial cells could also avoid immunoreactions [8,12,13]. Endothelial cells react to the shear stress through various mechanosensing systems such as ion channels, integrins, and cell junction molecules [14]. Unidirectional high shear stress induces anti-thrombogenic effects on the endothelial cell surface and prevents platelet aggregation and thrombus formation [15,16]. In this study, allogenic HAECs were chosen as model endothelial cells since they are arterial cells and react faster to shear stress stimulation than HUVECs [17]. For further clinical application, premature endothelial colony-forming cells (ECFCs) as population of endothelial progenitor cells can be isolated out of the TEVG-recipient's blood and serve as autologous cells. ECFCs can be expanded in vitro to cell numbers relevant for seeding the TEVG scaffolds and thus are a promising cell source [11].

In previous works, we presented a bioreactor system specially developed for vascular graft cultivation with multiple monitoring and conditioning functions [18,19]. To date, various groups have developed bioreactor designs for the pre-conditioning and culturing of seeded TEVGs. They primarily focus on modeling physiological conditions to enhance cell growth in vitro [7,10,20–25]. The design of such a perfusion and rotation bioreactor has to cover the environmental requirements of a biological system by providing efficient internal and external medium transport. Biochemical and physical parameters as well as cell vitality need to be controlled during cultivation. This requires a robust system setup and the possibility to reuse the bioreactor containment for several cultivation processes of TEVGs is desirable. Different kinds of TEVG bioreactor setups have been presented over the past decades, with perfusion bioreactors as the predominantly used model [7,26–28], and here compactness and cost-efficiency are essential features. Huang et al. [29] developed a bioreactor for uni- or bi-axial stress application on cultured TEVGs using a linear motor. Baba et al. [27] combined the possibility of automated cultivation with enough space for dynamic stretching with an in vivo-like culture chamber made of polydimethylsiloxane (PDMS). Online monitoring during dynamic cultivation was achieved by integration of a digital microscope into a disposable, low-cost bioreactor [25]. This system is highly modular with many adjustable parameters such as flow, pressure, pulse rate, and pulse frequency, including a micro-centrifugal pump to adjust venous and arterial pressure levels. Because of this flexibility, the system is denoted as VasculTrainer. It represents a typical flow and rotational perfusion bioreactor system that can induce mechanical stimulation on the growing structure due to pulsatile flow and the thus resulting shear stress. Other reactor systems feature online monitoring of cultivation factors such as glucose, lactate, pH, CO<sub>2</sub>, and O<sub>2</sub> to control metabolic activity, as implemented in the bioreactor system by Felder [30]. An imaging feature is also important to monitor the growth behavior of the cultured structure in vitro, and here ultrasound appears suitable, with a relatively high resolution [19].

Successful endothelialization of tubular scaffolds depends upon shear stress [31]. In the work presented here, the medium viscosity was increased by the addition of methyl cellulose (MC) for a higher dynamic viscosity of the fluid in the vessel [32]. This reduces the necessary flow rate to reach higher shear stress levels affecting the endothelial cells. Furthermore, the inner cross-section of the vascular graft was reduced by the implementation of a centrally positioned rod, which helped to reduce the necessary volume flow for targeted wall-near shear stress levels.

Since TE-structures cultivated *ex vivo* in bioreactors have to fulfill requirements comparable to those established in pharmaceutical drug development with specific regulations for such advanced therapy medicinal product (= ATMP), our bioreactor system was optimized recognizing the guidelines of the FDA [18,19,33]. The cultivation process in the bioreactor system, thus, was monitored by controlling sterility over the entire cultivation period.

Before cultivating in the bioreactor, experiments in flow slides are a suitable tool to assess the general impact of flow on endothelial cell behavior and morphology [11,34]. Here flow rates correlated with certain shear stress levels can easily be tested in a pre-implemented reaction container with a flat endothelial monolayer on a surface only coated with fibrinogen. A medium thickened with MC first in the flow slides and second in the bioreactor was used. Before, a non-Newtonian model for viscosity measurements was fitted to properly simulate the fluid properties. Computational fluid dynamics (CFD) using Comsol Multiphysics were performed, to simulate the fluid behavior in the flow slides and in the bioreactor geometry. Thus it is possible to correlate the necessary volume flow with the wall-near shear stress. Shear stress levels similar to a native human artery (10–15 dyn/cm<sup>2</sup>) should be reached in tubular scaffold geometry. The calculated necessary volume flow values were later applied in the bioreactor system to reach the target level of wall-near shear stress. Volume flow was controlled in the bioreactor by online intra-reactor-flow measurements using ultrasonic flow detection elements. CFD simulation is also suitable for identifying possible turbulences as well as non-uniform flow profiles in the reactor chamber during dynamic cultivation and localizing the affected areas of the cultivated TEVG surface. Following, microscopic analyses of the particular TEVG sections can be performed to determine the relevancy of those flow disturbances on the cell monolayer consistency.

The aim of the presented work was to develop a standardized dynamic cultivation protocol in a bioreactor system for the endothelialization of a scaffold, serving as a template structure for a future TEVG with flow-resistant and anti-thrombogenic surface properties. In this work, cultivation was conducted using a decellularized porcine artery seeded with HAECs. The cultivation continued over six days under controlled pressure and shear stress (stepwise raised to 10 dyn/cm<sup>2</sup>) conditions. Immunofluorescence staining was performed to confirm endothelialization and monolayer stability as well as alignment to the flow after perfusion.

## 2. Materials and Methods

### 2.1. Bioreactor system

#### 2.1.1. Design of the bioreactor system

The bioreactor system was designed to create an optimal environment for the cultivation of a tissue-engineered vascular graft (Fig. 1). The central element of the bioreactor system is the bioreactor chamber in which the tubular scaffold for the vascular graft is fixated (Fig. 1B). The current primarily used bioreactor setup is devised for vascular grafts with an inner diameter of up to 10 mm. The tubular scaffold was mounted between the two end covers of the bioreactor chamber over a section of 4 cm, that was seeded with cells. The total length of the native scaffolds used was up to 10 cm, and as a result, the overlapping ends were not seeded. The inner medium circulation leads through the vascular graft and simulates blood flow (total volume of 250 mL). The outer circulation fills the space surrounding the graft with a liquid medium, simulating the interstitial space in a biological system (total volume of 150 mL). Generally, the medium circulating was not exchanged throughout the total cultivation period. The cell culture medium is transported by two continuously running peristaltic pumps (Spetec GmbH, Erding, Germany), and a physiological pressure profile and flow rate can be applied by using a precision pressure control system (Biophysical Tools GmbH, Leipzig, Germany) connected to a pulse chamber. The flow rate is measured using a non-invasive ultrasonic flow sensor

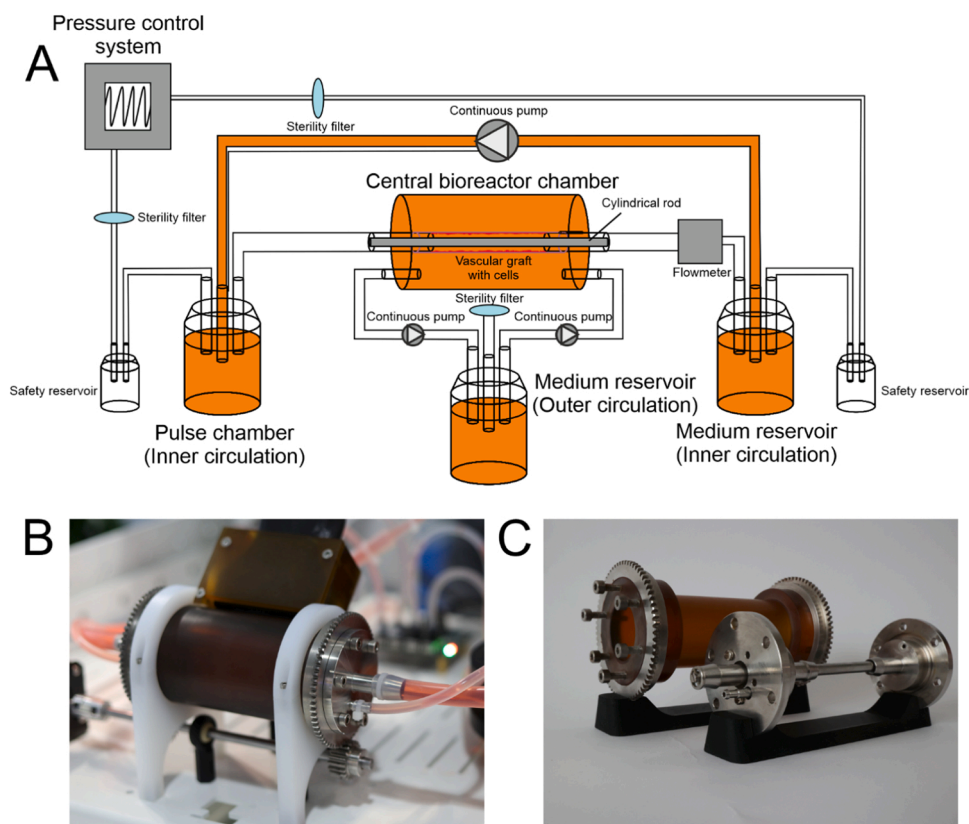


**Fig. 1.** : Bioreactor system. A: Schematic of the bioreactor setup. The bioreactor consists of two medium circuits. The inner circuit transports the medium through the vascular graft while the outer transport the medium around the graft. A pulsatile medium flow can be applied through the pulse chamber connected to a pressure control system. B: Central bioreactor chamber. C: Disassembled central bioreactor chamber with inserted cylindrical rod.

(Sonotec, Halle (Saale), Germany) and medium sampling takes place at the sample port (Safeflow, B. Braun SE, Melsungen, Germany). The bioreactor's fluid circuit is shown in Fig. 1A. An in-depth technical description of the bioreactor setup is given by Stanislawski et al., 2020 [19]. Only materials that are FDA or ISO10993 certified and meet USP Class VI: were used, e.g., the plastic polyetherimide for the bioreactor chamber, stainless, steel for the bioreactor chamber lids and the inserted rod, gas permeable silicone tubing, and glass for the medium reservoirs. As a new addition to the system, the cylindrical rod was inserted into the inner circuit of the central bioreactor chamber to increase medium flow speed and therefore wall-near shear stress in this section (Fig. 1C).

The bioreactor system can generally be used within the following limits for different parameters: the pressure system can apply pressure ranging from  $-500$  mbar and  $500$  mbar to the pulse chamber and the medium reservoir. Different flow rates of up to  $400$  mL/min through the bioreactor chamber can be achieved depending on the set pressure difference between the pulse chamber and the medium reservoir. In contrast, the mean flow rate must not exceed  $\sim 280$  mL/min which is the maximum of the continuous pump. The pressure can also be regulated by a periodic function in the control software, which allows the application of varying pressure during cultivation in addition to fixed pressure settings.

### 2.1.2. Sterility evaluation of the bioreactor system

The bioreactor setup was generally designed for non-contact operation and simple assembly to ensure sterility. All parts were autoclaved at  $121$  °C,  $2$  bar for  $20$  min. After assembly in a laminar flow cabinet, the complete construct was autoclaved a second time before the vascular graft and the cylindrical rod with a  $6$  mm diameter were inserted and the cell culture medium was added to the circuit. In- and outgoing tubes connected to the pressure system are kept sterile using sterility filters.

Peristaltic pumps and the flow meter are connected to the tubing externally.

Since contamination of the cell culture medium and thus of the vascular prosthesis poses a life-threatening risk after implantation into patients, the medium was also carefully tested for bacterial contamination after the cultivation process. Testing of the re-seeded decellularized porcine artery (see Section 2.4.3) was performed using a Microsart RESEARCH Bacteria Kit (Sartorius Stedim, Göttingen, Germany) according to the manufacturer's instructions.

## 2.2. Pre-requisites for dynamic cultivation

### 2.2.1. Medium thickening and viscosity measurement

To increase wall-near shear stress within the given wide geometry of the tubular vascular scaffold used in this work, the viscosity of the cell culture medium EGM-2 (see Section 2.4.1) was increased by the addition of methyl cellulose (MC; M7027 Sigma-Aldrich, St. Luis, USA). MC was autoclaved before addition to the cell culture medium. For flow experiments and dynamic cultivation in the bioreactor system, the medium was pre-heated to  $37$  °C, mixed with MC, and stirred, before the solution was stored at  $4$  °C overnight to ensure that the total MC was dissolved.

The viscosity of the cell culture solutions containing varying concentrations of MC ( $0\%$ ,  $0.5\%$ ,  $1\%$ ,  $1.5\%$ , and  $2\%$ ) was measured using a parallel-plate viscometer (MCR 302, Anton Paar, Ostfildern-Scharnhausen, Germany) with a planar probe and a diameter of  $39.980$  mm (PP40). A pre-heated sample volume of  $670$   $\mu$ L was used. The gap between the probe and the plate was set to  $0.5$  mm. All measurements were performed at  $37$  °C. The samples were tested logarithmically at shear rates from  $10$  to  $1000$   $s^{-1}$  including the point of greatest physiological interest up to  $300$   $s^{-1}$ . For each tested shear rate  $15$  measurements with a measuring time of  $10$ – $6$  s were performed.

Based on viscosity measurements of the used thickened medium, a non-Newtonian power law model was programmed for each sample with the following equation

$$\mu = m * \max(\dot{\gamma}, \dot{\gamma}_{\min})^{n-1} \quad (1)$$

with flow consistency coefficient  $m$ , flow behavior index  $n$ , viscosity  $\mu$ , shear rate  $\dot{\gamma}$ , and the lower shear rate limit  $\dot{\gamma}_{\min}$ .

### 2.2.2. Shear stress estimation

The shear stress acting on the inner wall of the cultured graft inside the bioreactor system or comparatively in  $\mu$ -slides 0.8 I Luer (uncoated, 0.8 mm channel height, ibidi, Gräfelting, Germany) was estimated by performing a CFD simulation using Comsol Multiphysics 5.2. The following settings were used for the simulation: a laminar fluid model for incompressible flow; a boundary condition with a flow set to zero; a non-Newtonian power law model (Eq. 1) as viscosity model; GMRES as a linear solver (details in the Supplementary Table S1). The parameters for the viscosity model were adapted from the rheological measurements presented in Section 3.1. The laminar inflow was defined based on calculations for water at 20 °C, with a volume flow of 300 mL/min, in a pipe with a diameter of 8 mm. The volume flow was within the Reynolds laminar range with a value of 789; a higher viscosity of MC-medium would reduce the Reynolds number. The laminar inflow was varied between 0.1 and 10 mL/min for the flow slides and 50 and 300 mL/min for the bioreactor system. The shear stress was evaluated by averaging it across the central area of the flow slide and the vascular graft (areas are indicated in Fig. 3). Results for the flow slides were compared to the formula given by ibidi, and results for the bioreactor system were interpolated using a linear function (Eq. 3).

To control the shear stress during cultivation in the bioreactor system, the minimum, the mean, and the maximum flow rates measured with the flow sensor during cultivation experiments, were converted to the corresponding shear stress values using Eq. 3.

## 2.3. Cell culture

### 2.3.1. Primary cells

During all experiments, cells from passages four to six were used. Human aortic endothelial cells (HAEC; Lonza, Cologne, Germany) were cultivated in EGM-2 (PromoCell, Heidelberg, Germany), supplemented with associated supplement mix, additional 8% FCS (Capricorn Scientific GmbH, Erbsdorfergrund, Germany) and 0.5% gentamycin (Biochrome, Berlin, Germany), at 37 °C with 5% CO<sub>2</sub> and 20% O<sub>2</sub>.

### 2.3.2. Assessment of metabolic activity

Metabolic activity of cells was generally assessed using the Cell Titer Blue assay (=CTB assay). This was specially performed to test possible effects of MC-thickened medium on HAECs as model cells. HAECs were seeded before the CTB assay in a 96-well plate with a density of 10.000 cells/well in 100  $\mu$ L cell culture medium. After 24 h, the medium was replaced by thickened medium containing varying concentrations of MC (0%, 0.5%, 1%, 1.5%, 2%). Each sample was assigned to four wells. After 24 h of incubation with MC, the samples were replaced by the CTB reagent in basal medium and incubated for one hour. The metabolic activity of the cells was measured by the reduction of resazurin to resorufin. The fluorescence of resorufin is measured at 597/584 (Ex./Em.). Cells in contact with MC were compared to cells cultivated without MC.  $N = 3 * 4$  samples per MC concentration.

### 2.3.3. Static and dynamic cultivation in flow slides

Shear stress experiments were performed using  $\mu$ -slides 0.8 I Luer (uncoated, 0.8 mm channel height, ibidi, Gräfelting, Germany). The slides were coated with fibrinogen (Sigma-Aldrich, St. Luis, USA) diluted 50  $\mu$ g/mL in PBS (NaCl, Roth, Karlsruhe, Germany) and incubated for 1 h at room temperature. After washing with PBS and rinsing with EGM-

2, the slides were seeded with  $3.5 \times 10^5$  HAECs ( $1.4 * 10^5$  cells/cm<sup>2</sup>). After 3 h of incubation at 37 °C, 20% O<sub>2</sub> and 5% CO<sub>2</sub> allowing cell adhesion, non-adherent cells were carefully rinsed out with EGM-2 containing additional 1% MC. Slides were exposed to either static (0 dyn/cm<sup>2</sup>) or dynamic conditions to create a high level of shear stress using pulsatile flow (10 dyn/cm<sup>2</sup>). For the dynamic cultivation, slides were connected to a perfusion system (ibidi) following the manufacturer's instructions and cultivated under static conditions for 21 h before a quasi-static flow was applied with shear stress < 0.5 dyn/cm<sup>2</sup> for another 24 h. Then the shear stress was gradually raised to 10 dyn/cm<sup>2</sup> (with intermediate levels of 2.5, 5, and 7.5 dyn/cm<sup>2</sup> over 48 h). Dynamic cultivation with 10 dyn/cm<sup>2</sup> and a pulse of 1 Hz was prolonged for another 48 h before cells were fixated with 4% paraformaldehyde (PFA). Flow rates for targeted shear stress were calculated according to Eq. 2 provided by ibidi<sup>2</sup> and are given in Table 1. Shear stress was also estimated using Comsol Multiphysics resulting in comparable values (data not shown). For the static condition, slides were cultivated over 120 h with a daily exchange of medium with 1% MC. After fixation, slides with cells were further subjected to immunohistochemistry.

$$\text{shear stress} = (m * \dot{\gamma}^{n-1}) * 34.7 * \text{flow rate} \quad (2)$$

### 2.3.4. Dynamic cultivation of xenogenous TEVG in the bioreactor system and static control

Decellularized porcine arteries (biotrics bioimplants AG, Berlin, Germany, diameter ~10 mm) were re-seeded using HAECs. A volume of 26 mL of cell solution ( $0.5 * 10^6$  cells/mL cell culture medium,  $\sim 2.0 * 10^5$  cells/cm<sup>2</sup>) was used for seeding. EGM-2 containing 1% of MC was used during cultivation. The solution was filled into the porcine artery, which was fixed inside the central bioreactor chamber with the cylindrical rod (diameter 6 mm). The chamber was rotated with an alternate motion + / - 180° with a frequency of 1/24 Hz (equivalent to 5 complete rotations per minute) for 6 h to allow the cells to attach equally to the whole inner surface of the scaffold; then, the cell solution was substituted with fresh medium. After an additional 18 h of rotation, defined pressure was applied to the medium to achieve the defined flow rate in the inner circulation of the bioreactor. The re-seeded porcine artery was cultivated at 37 °C in an atmosphere of 5% CO<sub>2</sub> and 20% O<sub>2</sub> inside the bioreactor system, and cultivation was prolonged for additional six days with continued rotation. Under estimated quasi-static cultivation conditions based on Comsol simulation, a laminar flow of up to 15 mL/min was induced after the first 24 h, equivalent to a shear stress of up to 0.5 dyn/cm<sup>2</sup>. To establish dynamic cultivation conditions with a target shear stress of 10 dyn/cm<sup>2</sup> after the quasi-static cultivation of 24 h, pressure in the pulse chamber and, therefore, the flow rate was stepwise increased to reach a wall-near shear stress of 7.5 dyn/cm<sup>2</sup> in the TEVG. On this hydrodynamic level, a pressure pulse with a frequency of 1 Hz was applied to the pulse chamber (Eq. 3) provoking a

**Table 1**

Flow rates and resulting shear stress. Flow rates used during the cultivation in flow slides (0.8 mm) and estimated shear stress values (based on Eq. 2 and verified using CFD simulation (Section 2.3.2)).

| Condition         | Flow rate [mL/min] | Estimated shear stress [dyn/cm <sup>2</sup> ] |
|-------------------|--------------------|---|
| Static            | 0                  | 0   |
| Quasi-static      | < 0.3              | < 0.5   |
| Dynamic           | 1.8                | 2.5   |
| Dynamic           | 4.0                | 5   |
| Dynamic           | 6.3                | 7.5   |
| Dynamic pulsatile | 8.6                | 10  |

<sup>2</sup> [https://ibidi.com/img/cms/support/AN/AN11\\_Shear\\_stress.pdf](https://ibidi.com/img/cms/support/AN/AN11_Shear_stress.pdf)



medium pulse wave with a peak flow rate of 313 mL/min to achieve a wall-near shear stress of 10 dyn/cm<sup>2</sup>.

$$pressure = \sin(2\pi t) * 550\text{mbar} + 330\text{mbar} \quad (3)$$

The pulsatile flow was continued over 48 h until the end of the cultivation. The complete pressure settings and the resulting flow rates are displayed in Table 2. Shear stress values were calculated using Eq. 5 based on CFD simulation (see Sections 2.3.2 and 3.2).

As a static control, sections of a decellularized porcine artery (1 × 1 cm) were seeded with 0.5 × 10<sup>6</sup> HAECs/cm<sup>2</sup>. Therefore, sections were placed in a 6-well plate and 100 µL EGM-2 containing the cells was carefully pipetted on the surface of each section. The sections were placed in an incubator at 37 °C, 20% O<sub>2</sub> and 5% CO<sub>2</sub> for one hour before adding 4 mL medium to each well. Cultivation was prolonged for six days with a medium exchange after three days.

## 2.4. Evaluation of static and dynamic cultivation

### 2.4.1. Immunohistochemistry and image acquisition

After cultivation, the seeded porcine artery used as a scaffold was fixed with 4% PFA for 30 min at RT and washed with phosphate buffer saline (PBS). Small Section (5×5 mm) of the *tunica intima* were prepared before staining. VE-cadherin was stained by incubating the tissue with a primary antibody (Abcam, Cambridge, UK; dilution 1:500) overnight at 6–8 °C and subsequently for two days at 6–8 °C with a secondary antibody (Abcam, Cambridge, UK; dilution 1:2000). Afterwards, an actin skeleton staining was performed by incubation for one hour at RT with phalloidin (Abcam, Cambridge, UK; dilution 1:1000). Cell nuclei were stained using Hoechst 33342 (Thermo Fisher Scientific, Waltham, USA). Between each step, tissue slices were extensively washed with PBS. Tissue sections were placed between two glass slides, and images were taken using a Leica TCS SP5 and a Leica TCS SP8 confocal microscope (Leica Microsystems GmbH, Wetzlar, Germany). Z-stacking enhanced the picture quality of curved scaffold sections by z-projection.

### 2.4.2. Analysis of cell morphology

$$Roundness = \frac{4A}{\pi L^2} \quad (4)$$

Axis rotation and roundness were calculated from images after VE-cadherin staining and image processing including background subtraction, contrast enhancement, threshold adjustment, and object detection with ImageJ software (see Supplementary Fig. S4). Cell elongation was characterized using the parameter “roundness” (range 0 = straight line to 1 = circle) according to Brown [35] based on the formula:

Cell elongation was also assessed by calculation of the axis ratio between the longest and shortest axis (1 = circle), while the orientation was assessed by determining the angle between the longest axis and the direction of flow (min/max = −90/90; 0 = in the direction of flow). The algorithm used detected and analyzed 210–260 cells per image for the ibidi slides and 50–80 cells per image for the scaffold cultivations.

**Table 2**

Pressure values set in the pressure control software and resulting flow rate as well as the calculated shear stress.

| Condition         | Pressure [mbar] | Target flow rate [mL/min] | Estimated shear stress [dyn/cm <sup>2</sup> ] |
|-------------------|-----------------|---------------------------|---|
| Static            | 0               | 0                         | 0   |
| Quasi-static      | 8               | < 15                      | < 0.5   |
| Dynamic           | 30              | 72                        | 2.5   |
| Dynamic           | 85              | 152                       | 5   |
| Dynamic           | 155             | 233                       | 7.5   |
| Dynamic pulsatile | SeeEq. 4        | Peak flow rate 313        | 10  |

### 2.4.3. Detection of glucose consumption and lactate production

Total glucose consumption and lactate production was measured using the YSI 2950 Biochemistry Analyzer (YSI Inc., Yellow Springs, USA) in the medium supernatant after cultivation of the reseeded porcine artery presented here. Medium samples were taken from the sample port under sterile conditions and compared to samples taken before the cultivations.

## 2.5. Statistics

Statistical analysis was performed with XLSTAT using Shapiro-Wilk-Test and Levene-Test for testing normality and equality of variances. For multiple comparisons of the cultivation conditions, ANOVA was used followed by the Tukeys’ test for pairwise comparison with p = 0.01.

## 3. Results

### 3.1. Viscosity measurements

MC-thickened cell culture medium was used inside the vascular graft. To estimate the wall-near shear stress for given flow rates in the cultivated TEVG using CFD simulation, viscosity models were created based on viscosity measurements (n = 3) performed as outlined before. Adding MC drastically increased the viscosity and encouraged shear thinning behavior (Fig. 2). The parameters (flow consistency coefficient and flow behavior index) of the fitted curves of the power-law model (Eq. 1) depicted in Fig. 2 are given in Table 3. In addition, it was noticed, that foam formed by stirring was more stable in solutions with higher amounts of MC.

The effect of the additional 8% FCS in the cell culture medium was also assessed (see Supplementary Figs. S2 and S3). The difference between medium with and without additional FCS is negligible in comparison to the addition of MC to the cell culture medium.

### 3.2. Simulation of flow rate and shear stress

For cultivation of the HAECs in the bioreactor system and flow slides, the necessary flow rates to achieve 0.5, 2.5, 5, 7.5, and 10 dyn/cm<sup>2</sup> using EGM-2 with 1% MC for the given geometries were calculated using Comsol Multiphysics. A fixed value (ranging from 0.1 to 10 mL/min for the flow slides and 10–350 mL/min for the vascular graft) with laminar inflow was set for the flow rate. As expected, velocity profiles were uniform both at the central areas of the vascular graft in the bioreactor (Fig. 3, see top left) and in the flow slides (Fig. 3, see bottom left). As a

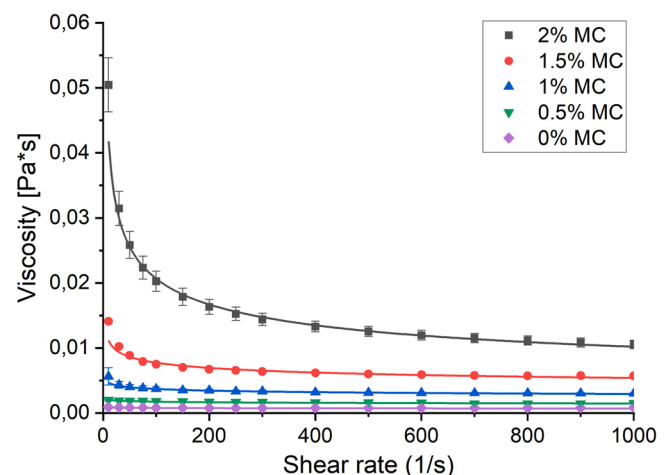


**Fig. 2.** Viscosity measurements. Viscosity measurements for cell culture medium (EGM-2) containing different concentrations of MC (0%, 0.5%, 1%, 1.5% and 2%) and corresponding fitted curves for shear stress estimation.

**Table 3**

Calculated parameters for the non-Newtonian power law model (Eq. 1) based on the viscosity measurements for cell culture medium containing varying concentrations of MC (0%, 0.5%, 1%, 1.5% and 2%).  $m$  = flow consistency coefficient,  $n$  = flow behavior index.

| MC   | $m$ (flow consistency coefficient) | $n$ (flow behavior index) |
|------|------------------------------------|---------------------------|
| 0%   | 0.00099                            | 0.9540                    |
| 0.5% | 0.00248                            | 0.9270                    |
| 1%   | 0.00592                            | 0.8994                    |
| 1.5% | 0.01592                            | 0.8441                    |
| 2%   | 0.08431                            | 0.6945                    |

consequence, nearly constant shear stress values resulted across the inner surface of the vascular graft and in the flow slides. A non-uniform flow was revealed near the inlet of the vascular graft (Fig. 3, top right). This is due to an outcropping of the xenogenous scaffold shortly after the narrow inlet of the bioreactor after fixing. Consequently, the simulation here shows variable shear stress in three small entry areas: first reduced shear stress ( $\sim 0$  cm, 2–4 dyn/cm<sup>2</sup>), then increased shear stress ( $\sim 0.1$  cm; 12–14 dyn/cm<sup>2</sup>), then reduced shear stress ( $\sim 0.2$  cm, 2–4 dyn/cm<sup>2</sup>). In the next section  $\sim 0.25$  cm behind the inlet, the shear stress is slightly elevated ( $\sim 12$  dyn/cm<sup>2</sup>). In the next section, starting at  $\sim 0.5$  cm, the shear stress is uniform until shortly before the outlet ( $\sim 10$  dyn/cm<sup>2</sup>). As expected, the shear stress distribution is also uniform across the entire central surface of flow slides (Fig. 3, bottom right) within its center (inner 3 mm with 1 mm distance to the side and 7.5 mm to inlet and outlet).

Shear stress calculated using Comsol Multiphysics for flow rates between 50 and 300 mL/min in the bioreactor system (Supplementary Fig. S1) resulted in a linear curve (Eq. 5).

$$\text{shear stress} = 0.031 * \text{flow rate} + 0.2805 \quad (5)$$

Results gained for flow slides were similar to calculations using Eq. 2.

The effect of the rotation of the central bioreactor chamber on the resulting shear stress was also analyzed using a modified simulation model. The effect of the slow rotation was shown to be very small in comparison to the shear stress resulting from the flow rate of the cell culture medium (Supplementary Fig. S6).

### 3.3. Assessment of metabolic activity

The effect of MC on the metabolic activity of endothelial cells was tested by assessing the metabolic activity of HAECs, cultivated with cell culture medium containing MC in a concentration up to 2% (w/v). The results of the CTB assay are displayed in Fig. 4. Adding MC to the cell

culture medium significantly increased the metabolic activity of HAECs. Maximal values were reached for 2% MC with an increase up to  $\sim 150\%$  versus control without MC. No decreasing effect of MC on the metabolic activity was observed.

### 3.4. Cultivation of HAECs in flow slides

To analyze the effect of shear stress on HAECs, the cells were seeded in ibidi flow slides and cultivated for six days under static (0 dyn/cm<sup>2</sup>) and dynamic pulsatile (10 dyn/cm<sup>2</sup>) conditions (Fig. 5). HAECs cultivated under static conditions display typical cobblestone-like morphology with irregular arrangements and no defined orientation (Fig. 6A). In contrast, after cultivation under dynamic pulsatile conditions with a maximum shear stress of 10 dyn/cm<sup>2</sup>, cell morphology is elongated, cell nuclei are slightly shifted, cells are aligned in the direction of flow (Fig. 6B), and cells form a confluent monolayer with only minor gaps. This effect can also be seen by comparing the orientation of the actin fibers. Under dynamic conditions, fibers are highly orientated parallel to the direction of flow while under static conditions, fibers

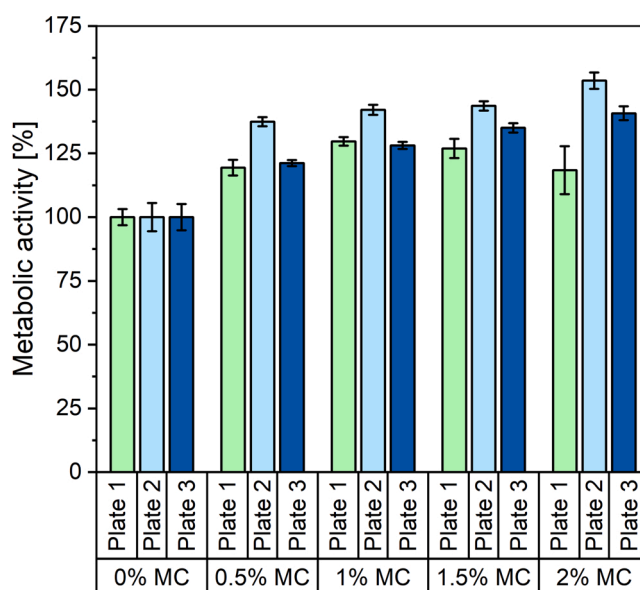


Fig. 4. Results of the CTB assay. The metabolic activity of HAECs was measured after 24 h of cultivation using a cell culture medium containing up to 2% MC (w/v);  $n = 4$  per plate, mean, standard error of the mean (SEM).

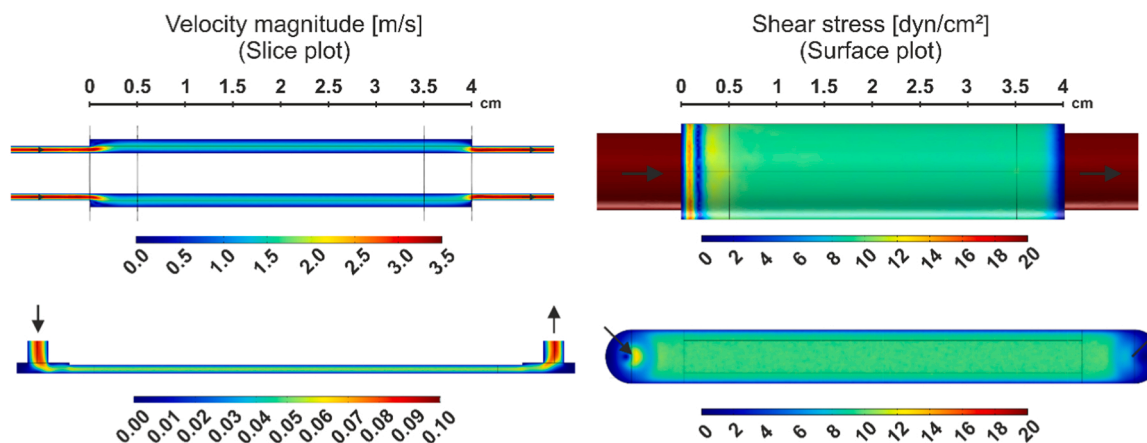
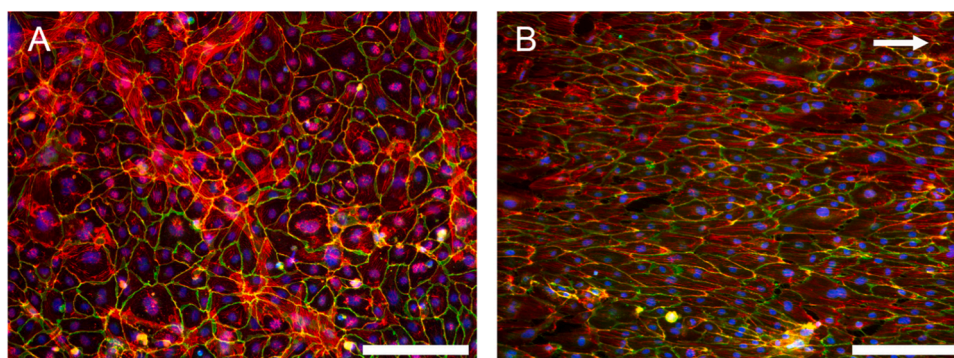
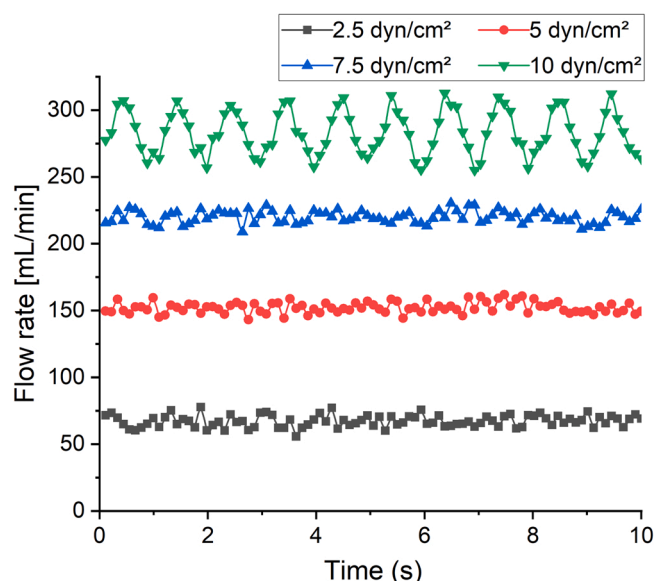


Fig. 3. : Simulation of velocity (left) and shear stress distribution on the inner surface (right) inside the central bioreactor chamber with inserted cylindrical rod (top) and at the bottom of the flow slides (bottom). Depicted results were calculated with a volume flow of 300 mL/min (bioreactor) and 8 mL/min (flow slide). Black arrows indicate the direction of flow. The shear stress level was homogeneous at  $\sim 10$  dyn/cm<sup>2</sup> in the inner areas of the bioreactor (0.5–3.5 cm) and in the flow slides.



**Fig. 5.** Endothelial monolayer (HAECs) after cultivation on flow slides for six days under static and dynamic conditions. A: Cells cultivated under static conditions ( $0 \text{ dyn/cm}^2$ ). B: Cells cultivated under dynamic pulsatile conditions ( $10 \text{ dyn/cm}^2$ ). The white arrow indicates the direction of flow. Cell nuclei are stained in blue (Hoechst 33342), cell-cell contacts are stained in green (VE-cadherin) and the cytoskeleton is stained in red (Phalloidin-iFluor 555). Scale bars indicate  $200 \mu\text{m}$ .



**Fig. 6.** : Measurements of medium flow during cultivation of the re-seeded porcine artery in the bioreactor system for different targeted shear stress conditions of  $2.5$ ,  $5$ ,  $7.5$ , and  $10 \text{ dyn/cm}^2$ .

display a chaotic pattern and grow partially on top of each other.

### 3.5. Cultivation of HAECs on porcine arteries in the bioreactor system

Three decellularized porcine arteries (aorta, diameter  $\sim 10 \text{ mm}$ ) were inserted in the bioreactor system before they were reseeded and cultivated under dynamic and pulsatile conditions (up to  $10 \text{ dyn/cm}^2$  on the inner surface of the vascular graft/ $1 \text{ Hz}$ ) for six days. During dynamic cultivation, the flow rate was stepwise increased to maximally  $313 \text{ mL/min}$ .

#### 3.5.1. Flow rate during the dynamic cultivation

The medium flow rate was constantly measured and recorded during pulsatile, dynamic cultivation in the bioreactor system. Measurements corresponding to conditions set to reach shear stress values of  $2.5$ ,  $5$ ,  $7.5$ , and  $10 \text{ dyn/cm}^2$  (according to CFD simulation) were analyzed (Fig. 5).

The mean flow rate was calculated for each measurement, and the minimum and maximum values were extracted. Based on Eq. 5, the estimated range of shear stress was calculated. (Table 4). The targeted flow rates were within the measured range of flow rates for the targeted conditions in the evaluated cultivation. Therefore, shear stress levels were in the range of the targeted shear stress levels, except for “Dynamic

**Table 4**

Measured flow rates during dynamic cultivation in the bioreactor system and corresponding calculated shear stress based on CFD simulation. Measured flow rates were converted into the corresponding shear stress levels and compared to the targeted shear stress levels according to CFD simulation (Eq. 5).

| Dynamic condition (Targeted shear stress levels according to CFD simulations) | Targeted flow rate [mL/min] (according to CFD simulations) | Measured flow rate Mean/Min/Max [mL/min] | Estimated shear stress levels, Mean/Min/Max [ $\text{dyn/cm}^2$ ] |
|---|--|--|---|
| $2.5 \text{ dyn/cm}^2$  | 72   | 67 / 56 / 78                             | 2.4 / 2.0 / 2.7   |
| $5 \text{ dyn/cm}^2$  | 152  | 152 / 143 / 162                          | 5.0 / 4.7 / 5.3   |
| $7.5 \text{ dyn/cm}^2$  | 233  | 220 / 209 / 230                          | 7.1 / 6.8 / 7.4   |
| Pulsatile $10 \text{ dyn/cm}^2$ , $1 \text{ Hz}$                              | Peak flow rate 313   | 283 / 255 / 313                          | 9.1 / 8.2 / 10.0  |

$7.5 \text{ dyn/cm}^2$ ” (slightly below the targeted value).

#### 3.5.2. Evaluation of endothelialization of porcine arteries with HAECs in the bioreactor system in comparison to a static control

After cultivation in the bioreactor system, tissue sections were examined microscopically using fluorescence staining for cell nuclei, VE-cadherin for cell-cell contacts, and phalloidin for the cytoskeleton (Fig. 7). Analysis of the fluorescence staining under dynamic conditions revealed a confluent monolayer of endothelial cells with a few minor gaps comparable to cell cultivation in flow slides, covering the graft on the inside (Fig. 7B). The presence of VE-cadherin indicates a tight connection of cells within a formed endothelium. Visual analysis of cell morphology revealed a significantly elongated shape of the HAECs, and cell alignment with cell nuclei shifted in the direction of flow in comparison to static cultivation (Fig. 7A) similar to HAECs cultivated under static and dynamic conditions in flow slides. We did microscopic analyses of sections taken in three areas with the non-uniform medium flow according to CFD simulations (Fig. 3) near the inlet of the graft. In the first area with reduced flow, the monolayer was incomplete with non-aligned cells with non-distinct cell-cell contacts (Fig. 7C). In the second area with increased flow and then drop-down to reduced flow, the cell layer was completely interrupted (Fig. 7D, left side), and following, VE-cadherin staining was reduced indicating decreased cell-cell contacts (Fig. 7D, right side). The complete rest of the endothelialized TEVG showed a continuous monolayer, as depicted in the exemplary image of Fig. 7B.

#### 3.6. Comparing quantitative analysis of cell morphology in flow slides and in the bioreactor system

In addition to the visual descriptive comparison of the cell



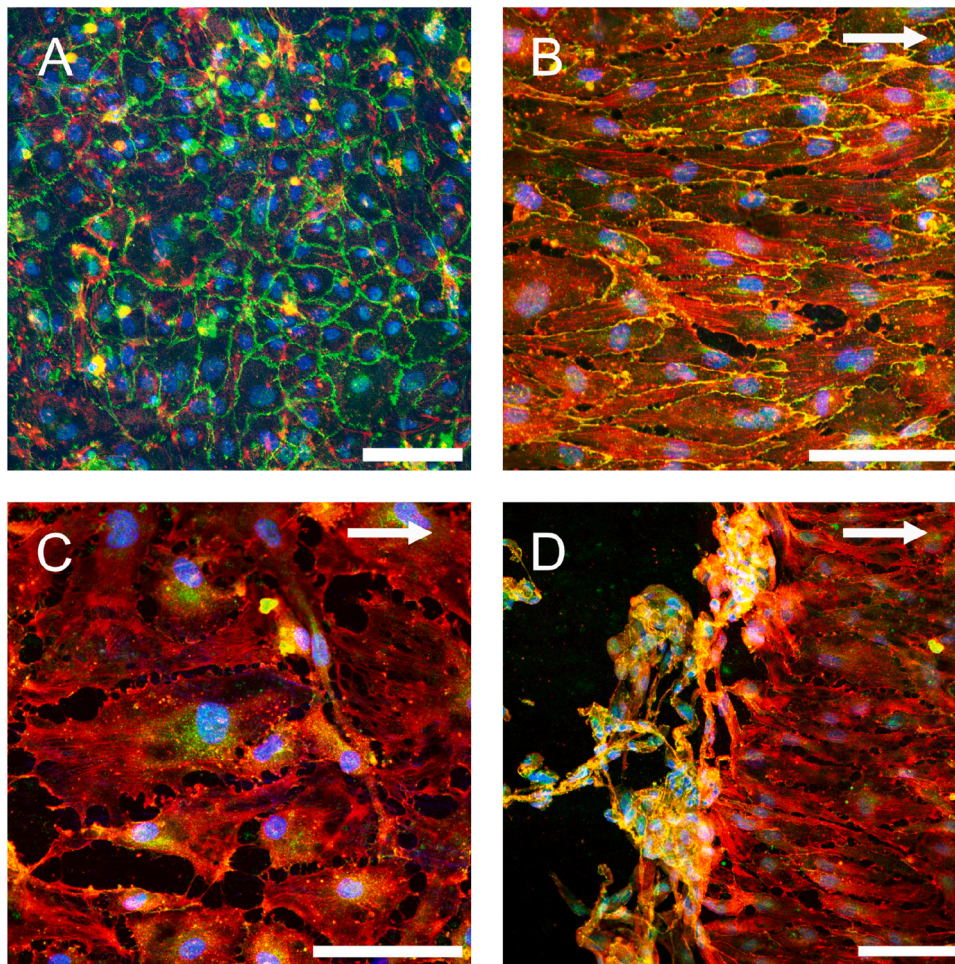


**Fig. 7.** : Endothelial monolayer (HAECs) after static cultivation and after dynamic pulsatile cultivation for six days inside the bioreactor system. A: Cells after static cultivation. B: Cells in the laminar flow area (0.5–3.5 cm in Fig. 3). C: Cells at the inlet near the connection to the bioreactor chamber with a non-uniform flow and low shear stress (0–0.1 cm in Fig. 3); D: Cells in the area with a non-uniform flow (0.1–0.3 cm in Fig. 3). Cell nuclei are stained in blue (Hoechst 33342), cell-cell contacts are stained in green (VE-cadherin), and the cytoskeleton is stained in red (Phalloidin-iFluor 555). Arrows indicate the direction of flow. Scale bars indicate 100  $\mu\text{m}$ .

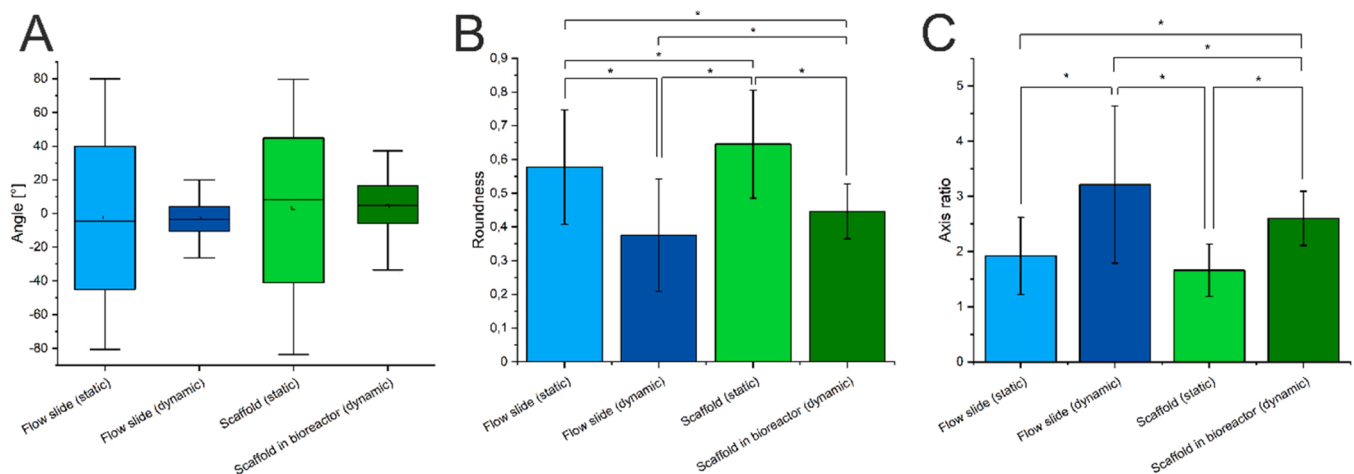


**Fig. 8.** : Mathematical assessment of HAEC-seeded flow slides and porcine artery sections. Cells were cultivated under static (light blue = control, static condition with 0  $\text{dyn}/\text{cm}^2$ ) or dynamic conditions (dark blue = dynamic/pulsatile condition with 10  $\text{dyn}/\text{cm}^2$ , 1 Hz) in flow slides and on porcine arteries under static (light green = static cultivation with 0  $\text{dyn}/\text{cm}^2$ ) or under dynamic conditions (dark green = dynamic, pulsatile conditions with 10  $\text{dyn}/\text{cm}^2$ , 1 Hz) in the bioreactor system for 6 days. A: Boxplots with values for the angle between cells and direction of flow; B: Roundness, calculated according to Eq. 4; C: Axis ratio.  $N = 3$  independent experiments with three sections per condition. \* $p < 0.01$  depicting significance according to ANOVA. Box plot: Box is determined by the 25th and 75th percentiles. The whiskers are determined by the 5th and 95th percentiles. Additionally, mean (dot) and median (line) values are displayed.



morphology, HAEC layers were analyzed mathematically by calculation of cell orientation (angle between the longest axis of the elongated cells and the direction of flow), roundness (according to Eq. 4), and axis ratio of the cells using cell outlines, stained with VE-cadherin. These parameters were determined in sections from the porcine artery cultivated under dynamic conditions in the bioreactor, and in statically cultured controls. For comparison HAECs cultivated in flow slides in the ibidi system under static (0 dyn/cm<sup>2</sup>) and dynamic and pulsatile conditions (10 dyn/cm<sup>2</sup>, 1 Hz) were also analyzed.

While cells cultivated under static conditions in ibidi slides displayed a random orientation, cells cultivated under dynamic conditions were highly orientated. This is represented by the distribution of the values presented in the boxplots (Fig. 8A). While the mean angle of orientation is near zero due to orientation in either a positive or negative direction, the range of the values differs greatly. Under static conditions, the range of the angles is significantly more extensive in the flow slides and on the porcine artery compared to dynamic cultivation in the slides and in the bioreactor system. This represents a random orientation of the cells from the static cultivations in contrast to an aligned orientation under dynamic conditions. The roundness of the HAECs in the flow slides was reduced from 0.58 to 0.38 under dynamic conditions; a roundness of 1 represents a perfect circle. The same observation was made for the HAECs seeded and cultivated on the porcine artery. The roundness was decreased from 0.65 to 0.45 under dynamic conditions (Fig. 8B). This was also confirmed by the axis ratio. Cells were clearly elongated, as the axis ratio shifted from 1.9 under static conditions to 3.2 under dynamic conditions in the flow slides and from 1.7 to 2.6 for cells cultivated on the porcine artery. When comparing the impact of dynamic cultivation in flow slides to the condition in the bioreactor system, a stronger effect is observed in the flow slides reflected by a decreased roundness and higher axis ratio. Furthermore, cells showed a significantly lower grade of roundness under static conditions on flow slides than on the porcine scaffold.

### 3.7. Monitoring of glucose/lactate

On day six of the dynamic cultivation of the reseeded porcine artery, glucose and lactate concentrations of the cell culture medium were measured using a YSI 2950 Biochemistry Analyzer (YSI Inc., Yellow Springs, USA). A consumption of 8.8% (w/v) of the initial glucose content of the medium was measured (=32.2 mg in total or 2.6 mg/cm<sup>2</sup> area of the TEVG). Lactate increased by 61.7 mg (4.9 mg/cm<sup>2</sup>).

### 3.8. Sterility evaluation

The sterility of the bioreactor system under continuous running without a cultivated graft was already proven [19]. Sterility testing was performed on day seven at the end of the cultivation of endothelial cells on a re-seeded decellularized porcine artery in the bioreactor system. No contamination was observed following qPCR analysis of the cell culture medium for bacterial 16 S rRNA.

## 4. Discussion

In this study, we developed a controlled endothelialization protocol for TEVGs by extra-corporal cultivation occurring under pulsatile flow conditions with shear stress up to 10 dyn/cm<sup>2</sup>. HAECs were used as model cells and decellularized porcine arteries as scaffolds. For cultivation, a TE-bioreactor system, with steady online control of volume flow and pressure, provided a monolayer development on the vascular scaffold [19].

Cultivation inside a suitable bioreactor can be referred to as “in situ tissue engineering”, and we consider this approach to be more successful than so-called “living bioreactors” with spontaneous implantation of a TEVG into a living organism for further seeding [36]. *In vitro*-created grafts represent highly complex functional implants suitable for a

plannable surgery. For optimization of TEVGs, various surface modifications for the synthetic materials have been tested and dynamic cultivation of colonized scaffolds prior to implantation appeared advantageous [37,38]. Other research groups treated TEVGs with stretching, stimulating collagen synthesis and smooth muscle cell proliferation. Therefore, dynamic cultivation is essential to induce anti-thrombogenic markers [11], and enhance biomechanical stability.

Visual analyses successfully proved the functionality of the newly presented endothelialization strategy in the bioreactor system. Endothelialization of a scaffold for a TEVG is critical since a confluent endothelial monolayer with high resistance against blood flow-induced shear stress is required to maintain a non-thrombogenic surface and thus represents a promising progression for sustainable vascular graft patency after implantation into a recipient [8]. The work presented here shows a suitable seeding and conditioning protocol with slowly increasing shear stress up to 10 dyn/cm<sup>2</sup> to prevent cell detachment and achieve complete endothelialization. A decellularized porcine artery served as an exemplary scaffold for cultivation, as this biomaterial surface is naturally composed [39]. In future cultivations, this porcine artery is to be replaced by a 3D-printed tubular scaffold structure. It might be in these future scenarios, that cells initially seeded get lost through the cultivation period. In this case, a non-invasive cell counting device could be used in future cultivations to monitor cell detachment [40].

Our cultivation protocol led to a successful formation of a nearly confluent endothelial monolayer with satisfying cell integrity on the entire inner surface of the porcine scaffold tube. Only small areas, localized near the inflow area of the tubular graft, showed incoherencies of the cell monolayer, which was correlated to non-uniform flow profiles according to Comsol CFD simulation. This result is very relevant, since monolayer integrity is strongly associated with the inhibition of platelet aggregation and the promotion of haemocompatibility [41]. Of course, these would be removed before the implantation of a vascular graft. Future grafts could also rely on more stable and standardizable 3D-printed tubular scaffold structures [42]. Here we expect non-uniform flow zones will be reduced because there would be no bloating due to the natural structure of the porcine scaffold.

With a pulsatile flow rate and shear stress up to 10 dyn/cm<sup>2</sup>, the experimental conditions chosen are comparable to the pressure conditions of a human artery and simulate wall-near shear stress in an arterial vessel [43,44]. The determined values for orientation, roundness and axis ratio from the cultivation in the bioreactor system were only slightly inferior to those detected in the miniaturized flow chamber system. Regarding the orientation, this might be due to the fact, that it was not possible to optimally align the porcine artery sections in the direction of flow in parallel to the horizontal camera axis during microscopy. Furthermore, evaluating each sample individually, the orientation variance is smaller than for all samples combined. This is also verified by the fact that each sample's mean orientation differs from zero more than the mean angle of all the samples together (see Supplementary Fig. S5). The stronger effect of the dynamic cultivation on the roundness and axis ratio of the endothelial cell cultivated in the flow slides can be explained by the different surface structure and properties of the slides in comparison to the porcine artery. The natural matrix of the artery enables a stronger adhesion of the endothelial cells due to more adhesion points, and a higher surface roughness compared to the fibrinogen coated flow slides. Therefore, the shear stress provoked a stronger response of the endothelial cells in flow slides than on the natural structure [45]. Nevertheless, in both dynamic cultivation setups (i.e., flow slide and bioreactor), a shift of the cell nuclei in the direction of flow was observed. This result is in line with results from other researchers [46, 47]. According to Tkachenko et. al., the polarization of the cells starts at shear stress > 7.2 dyn/cm<sup>2</sup> [48]. The orientation and order of the cytoskeleton shown by the actin stress fibers in the direction of flow in Figs. 6 and 7 are characteristic of a haemocompatible endothelial layer. Observations of others confirm, that a flow-directed alignment of HAECs occurs at a shear stress of 10 dyn/cm<sup>2</sup> and higher [44,49]. However,

achieving higher shear stress requires pre-conditioning and stepwise increasing to prevent cell detachment and destruction of the endothelial layer [8]. The presented timings in the cultivation protocol led to successful endothelialization of the central section of the vascular graft and are thus suitable for plannable and controlled TEVG generation in an extra-corporal cultivation containment over weeks.

We could show, that the utilized pressure system of the bioreactor used can be controlled to regulate physiological pressure and resulting flow rates. CFD simulations served as an estimation measure to calculate shear stress conditions inside the vascular graft and the flow slides using MC-thickened cell culture medium. As a basis for the correlation between the viscosity and the shear stress, we used the comparatively simple non-Newtonian power law model to describe the shear-thinning effect of MC. In the fitted regression curves, the  $R^2$  values are over 0.95 for all measurements (0–2.5% MC) with 0.98 for 1% MC. This indicates that the model was appropriate, and the use of a more complex model like the Carreau-model was not necessary. Simulations for the ibidi slides using Comsol resulted in similar shear stress values as given by the manufacturer for the respective flow chamber, therefore, confirming the created simulation model. In addition, the cell alignment similarity in both different dynamic cultivation approaches in ibidi and in the bioreactor verified the simulated shear stress values. According to the CFD simulations, a shear stress of 10 dyn/cm<sup>2</sup> could be reached using an MC concentration of 1% and a flow rate of 311 mL/min (bioreactor system) or 8 mL/min (flow slides). Thickening additives such as polysaccharides, e.g. xanthan gum and dextran can be negatively affected by autoclavation, whereas we found MC to be heat-sterilizable without losing its chemical and physical properties [50–53]. The results of the CTB assay showed that MC even had an increasing effect on the metabolic activity of the HAECs, which was in line with observations by Titze et al. for fibroblasts [54].

The intended biohybrid vascular graft is an advanced therapy medicinal product (ATMP) with approval processes comparable to those of a newly developed drug. To prepare a subsequent official approval of the final vascular graft in the future e. g. by the European Medicine Agency (EMA), this work thus aimed to reach compliance with national and international standards in drug development. Therefore, during the development of the vascular graft, attention was given to Good Manufacturing Practice, especially the harmonized regulations for ATMPs [55]. The cell culture medium was tested for bacterial contamination to check the sterility after successful cultivation. No bacterial contamination was observed. The use of Microsart® ATMP Sterile Release is targeted for future use, as this kit is already validated according to EP 5.1.6 (Alternative methods for control of microbiological quality) and EP 2.6.27 (Microbial Examination of cell-based Preparations) for contamination control of ATMPs and allows detection of almost all critical bacterial and fungal contaminations within three hours. Furthermore, we suggest adding human serum instead of fetal calf serum in EMA-approved protocols.

Previously presented cultivation protocols emphasized the importance of controlled glucose and lactate observation during cultivation. In addition, our group observed an increased glucose consumption by dynamically cultured (premature) endothelial cells and increased lactate production without pH shift [11]. The glucose rate here was comparably lower in HUVECs than in endothelial colony-forming cells, isolated from fresh human blood, a promising autologous cell source for future endothelialization protocols [11]. Although the glucose consumption of the HAECs was only 8.8% (32.2 mg) in six days, the predicted higher glucose uptake of available autologous cells must be considered for future cultivations and the overall concentration must be measured during cultivation. For the evaluation of the lactate levels throughout the cultivation, we would suggest using precise oxygen monitoring concerning diffusability across the scaffold barrier, especially when multi-cell layers on top of the scaffold are planned.

## 5. Conclusions

Altogether, the work presents a promising cultivation protocol in a bioreactor setup for dynamic vascular scaffold endothelialization. This could be useful as a standardized medical device and procedure for vascular ATMPs. For future vascular grafts, xenogenous decellularized scaffolds as used here may not be recommended, since these scaffolds provide a non-suppressible immune reactivity due to xenogenous residual cells and proteins with a stimulating effect on the immune system. They could be substituted by 3D printed, biodegradable polymer scaffolds [56]. Our work outlined the technical prerequisites for a fluid dynamic concept under sterile conditions with a balanced composition of medium viscosity, pressure control, and medium flow in the cultivated vascular graft. Successful vascular graft endothelialization under high shear stress conditions (10 dyn/cm<sup>2</sup>) with HAECs was achieved. The cells showed atheroprotective characteristics such as alignment in flow direction and lower roundness values.

## Funding Statement

This study was funded by the Deutsche Forschungsgemeinschaft [DFG – Grant Number: 388094931]. This work has been carried out within the framework of the SMART BIOTECS alliance between the Technische Universität Braunschweig and the Leibniz Universität Hannover. This initiative is supported by the Ministry of Economy and Culture (MWK) of Lower Saxony, Germany.

## CRediT authorship contribution statement

**Sebastian Heene:** Conceptualization, Data curation, Formal analysis, Investigation, Methodology, Software, Visualization, Writing – original draft. **Jannis Renzelmann:** Data curation, Formal analysis, Investigation, Methodology, Software, Writing – original draft. **Müller Caroline Müller:** Investigation. **Nils Stanislawski:** Software, Writing – review & editing. **Fabian Cholewa:** Methodology. **Pia Moosmann:** Resources. **Holger Blume:** Supervision, Writing – review & editing. **Cornelia Blume:** Conceptualization, Funding acquisition, Project administration, Resources, Supervision, Validation, Writing – original draft.

## Declaration of Competing Interest

The authors declare the following financial interests/personal relationships which may be considered as potential competing interests: Cornelia Blume reports financial support was provided by German Research Foundation. Cornelia Blume reports equipment, drugs, or supplies was provided by biotrics bioimplants AG, Berlin, Germany.

## Data Availability

Data will be made available on request.

## Acknowledgments

The authors thank Michaela Kreienmeyer and Prof. Dr. Theodor Doll (Department of Otorhinolaryngology, MHH) for optimal assistance and the opportunity to use the confocal microscopy systems. We thank Caroline Patterson as a native speaker with immense experience in scientific writing for help concerning the English style.

## Appendix A. Supporting information

Supplementary data associated with this article can be found in the online version at [doi:10.1016/j.bej.2023.109095](https://doi.org/10.1016/j.bej.2023.109095).

## References

- [1] G.A. Mensah, G.A. Roth, V. Fuster, The global burden of cardiovascular diseases and risk factors: 2020 and beyond, *J. Am. Coll. Cardiol.* 74 (2019) 2529–2532.
- [2] C.J.L. Murray, The global burden of disease study at 30 years, *Nat. Med.* 28 (2022) 2019–2026.
- [3] P. Gupta, B.B. Mandal, Tissue-Engineered vascular grafts: emerging trends and technologies, *Adv. Funct. Mater.* 31 (2021), 2100027.
- [4] C.E.T. Stowell, Y. Wang, Quickening: translational design of resorbable synthetic vascular grafts, *Biomaterials* 173 (2018) 71–86.
- [5] E.E. van Haaften, T.B. Wissing, M.C.M. Rutten, J.A. Bulsink, et al., Decoupling the effect of shear stress and stretch on tissue growth and remodeling in a vascular graft, *Tissue Eng. Part C. Methods* 24 (2018) 418–429.
- [6] D. Radke, W. Jia, D. Sharma, K. Fena, et al., Tissue engineering at the blood-contacting surface: a review of challenges and strategies in vascular graft development, *Adv. Healthc. Mater.* 7 (2018), e1701461.
- [7] A.J. Melchiorri, L.G. Bracaglia, L.K. Kimerer, N. Hibino, et al., In vitro endothelialization of biodegradable vascular grafts via endothelial progenitor cell seeding and maturation in a tubular perfusion system bioreactor, *Tissue Eng. Part C Methods* 22 (2016) 663–670.
- [8] H. Inoguchi, T. Tanaka, Y. Maehara, T. Matsuda, The effect of gradually graded shear stress on the morphological integrity of a huvec-seeded compliant small-diameter vascular graft, *Biomaterials* 28 (2007) 486–495.
- [9] J.D. Stroneck, L.C. Ren, B. Klitzman, W.M. Reichert, Patient-derived endothelial progenitor cells improve vascular graft patency in a rodent model, *Acta Biomater.* 8 (2012) 201–208.
- [10] T.-Y. Kang, J.M. Hong, B.J. Kim, H.J. Cha, et al., Enhanced endothelialization for developing artificial vascular networks with a natural vessel mimicking the luminal surface in scaffolds, *Acta Biomater.* 9 (2013) 4716–4725.
- [11] X. Kraus, M. Pflaum, S. Thoms, R. Jocznyk, et al., A pre-conditioning protocol of peripheral blood derived endothelial colony forming cells for endothelialization of tissue engineered constructs, *Microvasc. Res.* 134 (2021), 104107.
- [12] F. Copes, N. Pien, S. van Vlierberghe, F. Boccafroschi, et al., Collagen-based tissue engineering strategies for vascular medicine, *Front. Bioeng. Biotechnol.* 7 (2019), 166.
- [13] J.J. Glynn, M.T. Hinds, Endothelial outgrowth cells: function and performance in vascular grafts, *Tissue Eng. Part B, Rev.* 20 (2014) 294–303.
- [14] Y. Fang, D. Wu, K.G. Birukov, Mechanosensing and mechanoregulation of endothelial cell functions, *Compr. Physiol.* 9 (2019) 873–904.
- [15] K.-S. Heo, K. Fujiwara, J. Abe, Shear stress and atherosclerosis, *Mol. Cells* 37 (2014) 435–440.
- [16] D.A. Chistiakov, A.N. Orekhov, Y.V. Bobryshev, Effects of shear stress on endothelial cells: go with the flow, *Acta Physiol. (Oxf., Engl.)* 219 (2017) 382–408.
- [17] M.R. Maurya, S. Gupta, J.Y.-S. Li, N.E. Ajami, et al., Longitudinal shear stress response in human endothelial cells to atheroprotective and atheroprotective conditions, *Proc. Natl. Acad. Sci. USA* 118 (2021).
- [18] P. Maschhoff, S. Heene, A. Lavrentieva, T. Hentrop, et al., An intelligent bioreactor system for the cultivation of a bioartificial vascular graft, *Eng. Life Sci.* 17 (2017) 567–578.
- [19] N. Stanislawski, F. Cholewa, H. Heymann, X. Kraus, et al., Automated Bioreactor System for the Cultivation of Autologous Tissue-Engineered Vascular Grafts *Ann. Int. Conf. IEEE Eng. Med. Biol. Soc. IEEE Eng. Med. Biol. Soc. Annu. Int. Conf. 2020* 2257 2261.
- [20] H. Chen, J. Cornwell, H. Zhang, T. Lim, et al., Cardiac-like flow generator for long-term imaging of endothelial cell responses to circulatory pulsatile flow at microscale, *Lab Chip* 13 (2013) 2999–3007.
- [21] J. Eberth et al. US 2016/0298073 A1 Pulsatile Perfus. Bioreact. mimicking, Control., Optim. blood vessek Mech. 2016.US 2016/0298073 A1.
- [22] F.E.M. Herrmann, P. Lamm, P. Wellmann, S. Milz, et al., Autologous endothelialized vein allografts in coronary artery bypass surgery - Long term results, *Biomaterials* 212 (2019) 87–97.
- [23] N.M. Patel, R.K. Birla, Pulsatile flow conditioning of three-dimensional bioengineered cardiac ventricle, *Biofabrication* 9 (2016) 15003.
- [24] D.A. Prim, J.D. Potts, J.F. Eberth, Pulsatile perfusion bioreactor for biomimetic vascular impedances, *J. Med. Devices* 12 (2018).
- [25] F. Wolf, D.M. Rojas González, U. Steinseifer, M. Obdenbusch, et al., VasuTrainer: a mobile and disposable bioreactor system for the conditioning of tissue-engineered vascular grafts, *Ann. Biomed. Eng.* 46 (2018) 616–626.
- [26] V.I. Sevastianov, Y.B. Basok, A.M. Grigoryev, L.A. Kirsanova, et al., A perfusion bioreactor for making tissue-engineered constructs, *Biomed. Eng.* 51 (2017) 162–165.
- [27] K. Baba, A. Mikhailov, Y. Sankai, Combined automated culture system for tubular structure assembly and maturation for vascular tissue engineering, *JBSE* 13 (2018).
- [28] D. Wolf, K. Ley, Immunität und Entzündung bei Arteriosklerose, *Herz* 44 (2019) 107–120.
- [29] A.H. Huang, Y.-U. Lee, E.A. Calle, M. Boyle, et al., Design and use of a novel bioreactor for regeneration of biaxially stretched tissue-engineered vessels, *Tissue Eng. Part C Methods* 21 (2015) 841–851.
- [30] M.L. Felder, A.D. Simmons, R.L. Shambaugh, V.I. Sikavitsas, Effects of flow rate on mesenchymal stem cell oxygen consumption rates in 3D bone-tissue-engineered constructs cultured in perfusion bioreactor systems, *Fluids* 5 (2020) 30.
- [31] X. Kraus, E. van de Fliedert, J. Renzelmann, S. Thoms, et al., Peripheral blood derived endothelial colony forming cells as suitable cell source for pre-endothelialization of arterial vascular grafts under dynamic flow conditions, *SSRN J.* (2022).
- [32] J. Spangenberg, D. Kilian, C. Czichy, T. Ahlfeld, et al., Bioprinting of magnetically deformable scaffolds, *ACS Biomater. Sci. Eng.* 7 (2021) 648–662.
- [33] C. Leibold, J. Wilkening, C. Blume, H. Blume, A toolchain for the 3D-visualization of bioartificial vascular grafts based on ultrasound images. 2016 *IEEE Biomedical Circuits and Systems Conference (BioCAS)*. 2016 *IEEE Biomedical Circuits and Systems Conference (BioCAS)*, Shanghai, China, 17.10.2016 - 19.10.2016, IEEE, 2016, pp. 115–118.
- [34] X. Kraus, E. van de Fliedert, J. Renzelmann, S. Thoms, et al., Peripheral blood derived endothelial colony forming cells as suitable cell source for pre-endothelialization of arterial vascular grafts under dynamic flow conditions, *Microvasc. Res.* 143 (2022), 104402.
- [35] M.A. Brown, C.S. Wallace, M. Angelos, G.A. Truskey, Characterization of umbilical cord blood-derived late outgrowth endothelial progenitor cells exposed to laminar shear stress, *Tissue Eng. Part A* 15 (2009) 3575–3587.
- [36] N. Dahan, U. Sarig, T. Bronshtein, L. Baruch, et al., Dynamic autologous reendothelialization of small-caliber arterial extracellular matrix: a preclinical large animal study, *Tissue Eng. Part A* 23 (2017) 69–79.
- [37] L. E. Niklason, R. S. Langer, Advances in tissue engineering of blood vessels and other tissues, *Transpl. Immunol.* 5 (1997) 303–306.
- [38] J. Luo, L. Qin, L. Zhao, L. Gui, et al., Tissue-engineered vascular grafts with advanced mechanical strength from human iPSCs, *Cell Stem Cell* 26 (2020) 251–261.e8.
- [39] U. Böer, L.G. Hurtado-Aguilar, M. Klingenberg, S. Lau, et al., Effect of intensified decellularization of equine carotid arteries on scaffold biomechanics and cytotoxicity, *Ann. Biomed. Eng.* 43 (2015) 2630–2641.
- [40] I. Havlik, K.F. Reardon, M. Ůnal, P. Lindner, et al., Monitoring of microalgal cultivations with on-line, flow-through microscopy, *Algal Res.* 2 (2013) 253–257.
- [41] X. Dong, X. Yuan, L. Wang, J. Liu, et al., Construction of a bilayered vascular graft with smooth internal surface for improved hemocompatibility and endothelial cell monolayer formation, *Biomaterials* 181 (2018) 1–14.
- [42] T. Baroth, S. Loewner, H. Heymann, F. Cholewa, et al., An intelligent and efficient workflow for path-oriented 3D bioprinting of tubular scaffolds, *3D Print. Addit. Manuf.* (2023).
- [43] B.J. Ballermann, A. Dardik, E. Eng, A. Liu, Shear stress and the endothelium, *Kidney Int. Suppl.* 67 (1998) S100–S108.
- [44] F.W. Charbonier, M. Zamani, N.F. Huang, Endothelial cell mechanotransduction in the dynamic vascular environment, *Adv. Biosyst.* 3 (2019).
- [45] S. Cai, C. Wu, W. Yang, W. Liang, et al., Recent advance in surface modification for regulating cell adhesion and behaviors, *Nanotechnol. Rev.* 9 (2020) 971–989.
- [46] H.-W. Lee, J.H. Shin, M. Simons, Flow goes forward and cells step backward: endothelial migration, *Exp. Mol. Med.* 54 (2022) 711–719.
- [47] A.-C. Vion, T. Perovic, C. Petit, I. Hollfinger, et al., Endothelial cell orientation and polarity are controlled by shear stress and VEGF through distinct signaling pathways, *Front. Physiol.* 11 (2020), 623769.
- [48] E. Tkachenko, E. Gutierrez, S.K. Saikin, P. Fogelstrand, et al., The nucleus of endothelial cell as a sensor of blood flow direction, *Biol. Open* 2 (2013) 1007–1012.
- [49] N. Baeyens, S. Nicoli, B.G. Coon, T.D. Ross, et al., Vascular remodeling is governed by a VEGFR3-dependent fluid shear stress set point, *eLife* 4 (2015).
- [50] A.M. Walker, C.R. Johnston, D.E. Rival, On the characterization of a non-Newtonian blood analog and its response to pulsatile flow downstream of a simplified stenosis, *Ann. Biomed. Eng.* 42 (2014) 97–109.
- [51] C.N. van den Broek, R.A.A. Pullens, O. Frøbert, M.C.M. Rutten, et al., Medium with blood-analog mechanical properties for cardiovascular tissue culturing, *Biorheology* 45 (2008) 651–661.
- [52] F. Munarin, S. Bozzini, L. Visai, M.C. Tanzi, et al., Sterilization treatments on polysaccharides: effects and side effects on pectin, *Food Hydrocoll.* 31 (2013) 74–84.
- [53] E. Hodder, S. Duin, D. Kilian, T. Ahlfeld, et al., Investigating the effect of sterilisation methods on the physical properties and cytocompatibility of methyl cellulose used in combination with alginate for 3D-bioplotting of chondrocytes, *J. Mater. Sci. Mater. Med.* 30 (2019), 10.
- [54] I.R. Titze, S.A. Klemuk, X. Lu, Adhesion of a monolayer of fibroblast cells to fibronectin under sonic vibrations in a bioreactor, *Ann. Otol. Rhinol. Laryngol.* 121 (2012) 364–374.
- [55] European Commission - Health and consumer directorate-general (Ed.), *EudraLex - The rules governing medicinal products in the European Union - Volume 4: Good Manufacturing Practice (GMP) guidelines*, Brussels.
- [56] C. Blume, X. Kraus, S. Heene, S. Loewner, et al., Vascular implants – new aspects for in situ tissue engineering, *Eng. Life Sci.* 22 (2022) 344–360.